Yonago Acta Medica 2020;63(3):154–162 doi: 10.33160/yam.2020.08.003 *Original Article*

Oligopeptide Transporter-1 is Associated with Fluorescence Intensity of 5-Aminolevulinic Acid-Based Photodynamic Diagnosis in Pancreatic Cancer Cells

Hidehito Kinoshita, Tsutomu Kanda, Tomoaki Takata, Takaaki Sugihara, Yukari Mae, Taro Yamashita, Takumi Onoyama, Yohei Takeda and Hajime Isomoto

Division of Gastroenterology and Nephrology, Department of Multidisciplinary Internal Medicine, School of Medicine, Faculty of Medicine, Tottori University, Yonago 683-8504, Japan

ABSTRACT

Background The 5-aminolevulinic acid (ALA)-based photodynamic diagnosis is based on the accumulation of photosensitizing protoporphyrin IX in the tumor after ALA administration. However, the mechanisms connecting exogenous ALA and tumor fluorescence in pancreatic cancer remain unclear. We aimed to elucidate the mechanism underlying the ALA-induced fluorescent.

Methods Human pancreatic duct epithelial cells (hPDECs) and pancreatic cancer cell lines were used. The expressions of ALA-associated enzymes and membrane transporters in these cell lines were investigated. ALA-induced fluorescence was also investigated.

Results The expression of oligopeptide transporter-1 (PEPT-1), through which ALA is absorbed, was significantly higher in AsPC-1 cells and lower in MIA PaCa-2 cells than in hPDECs. AsPC-1 cells showed rapid and intense fluorescence after ALA administration, and that was attenuated by PEPT-1 inhibition. ALA-induced fluorescence was not sufficiently strong in MIA PaCa-2 cells to distinguish the cells from hPDECs.

Conclusion We revealed the association of PEPT-1 with ALA-induced fluorescence. Cancers expressing PEPT-1 could be easily distinguished by this technique from normal cells. These findings help develop novel diagnostic modalities for pancreatic cancer.

Key words fine needle aspiration; oligopeptide transporter-1; pancreatic cancer; photodynamic diagnosis; protoporphyrin IX

Pancreatic cancer is one of the leading causes of cancer-related deaths worldwide. Resection is still the only curative treatment for pancreatic cancer, however most patients cannot undergo curative resection because pancreatic cancer is difficult to detect at an early stage. In many cases, the cancer has already locally advanced or spread to other parts of the body, therefore curative resection cannot be performed.[1–4] Furthermore, the 5-year survival rate after curative resection is approximately 15–20%, with a median survival of 16–23 months.[5–8] Although the 5-year survival rate in pancreatic cancers at a size of less than 10mm was more than 80% in Japan, only 0.8% could be detected at this size.[9] Therefore, development of a novel diagnostic modality for identifying pancreatic cancer at an early stage is necessary.

Photodynamic diagnosis (PDD) is an optical imaging technology that involves the administration of photoactive drugs that selectively accumulate in the malignant tumor, resulting in drug-induced fluorescence.[10, 11] 5-aminolevulinic acid (ALA) is a precursor of photosensitizing protoporphyrin IX (PpIX) in the heme biosynthesis pathway. Exogenously administrated ALA increases the cellular PpIX levels, leading to an evident emission of red fluorescence at around 635 nm in certain tumors compared to the non-tumor surrounding tissues with a blue-violet excitation light.[10–12] Thus, ALA-PDD relies on tumor-specific PpIX accumulation. This technique has been applied for the detection of bladder and brain tumors.[11, 13] However, the utility of PDD has not been established for pancreatic cancer.

The heme biosynthesis pathway comprises eight consecutive enzymes (Fig. 1): 5-aminolevulinic acid synthase (ALAS), porphobilinogen synthase (PBGS), porphobilinogen deaminase (PBGD), uroporphyrinogen III synthase (UROS), uroporphyrinogen III decarboxylase (UROD), coproporphyrinogen oxidase (CPOX), protoporphyrinogen IX oxidase (PPOX), and ferrochelatase (FECH).[14] In addition to these enzymes, several transporters are also involved in the biosynthesis

Corresponding author: Tomoaki Takata, MD, PhD
t-takata@tottori-u.ac.jp
Received 2020 April 24
Accepted 2020 May 19
Online published 2020 June 12

Abbreviations: ABC, ATP-binding cassette; ALA, 5-aminolevulinic acid; ALAS, 5-aminolevulinic acid synthase; ANOVA, analysis of variance; CPOX, coproporphyrinogen oxidase; EUS-FNA, endoscopic ultrasound-guided fine needle aspiration; FBS, fetal bovine serum; FECH, ferrochelatase; hPDEC, human pancreatic duct epithelial cell; HRP, horseradish peroxidase; PBGD, porphobilinogen deaminase; PBGS, porphobilinogen synthase; PDD, photodynamic diagnosis; PEPT-1, oligopeptide transporter-1; PpIX, protoporphyrin IX; PPOX, protoporphyrinogen IX oxidase; RT, reverse transcript; UROD, uroporphyrinogen III decarboxylase; UROS, uroporphyrinogen III synthase

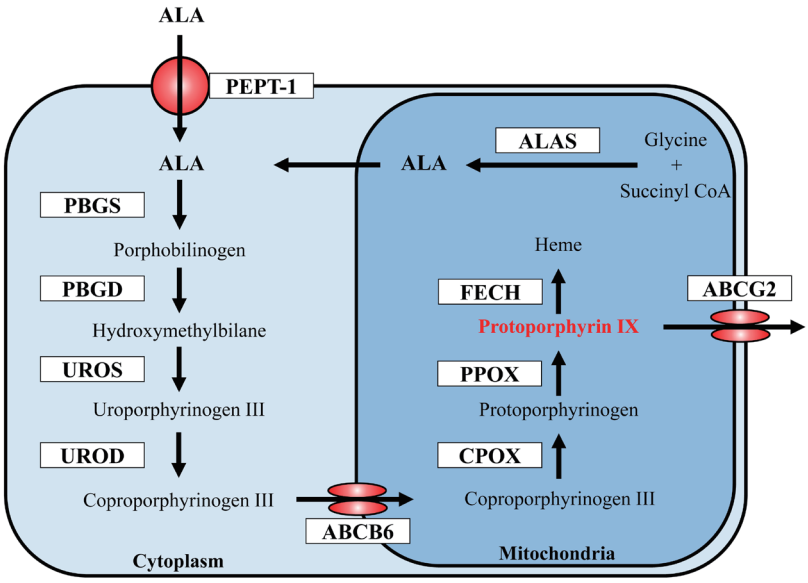

Fig. 1. Scheme of the heme biosynthesis pathway and membrane transporters. ALA is synthesized from glycine and succinyl CoA endogenously or exogenously absorbed through PEPT-1. Protoporphyrin IX synthesized from ALA via enzymatic reactions, then catabolized to heme by FECH or eliminated through ABCG2. ABC, ATP-binding cassette; ALA, 5-aminolevulinic acid; ALAS, 5-aminolevulinic acid synthase; CPOX, coproporphyrinogen oxidase; FECH, ferrochelatase; PBGD, porphobilinogen deaminase; PBGS, porphobilinogen synthase; PEPT-1, oligopeptide transporter-1; PPOX, protoporphyrinogen IX oxidase; UROD, uroporphyrinogen III decarboxylase; UROS, uroporphyrinogen III synthase.

and catabolism of heme and porphyrin, including oligopeptide transporter-1 (PEPT-1), and the ATP-binding cassette (ABC) transporters ABCB6 and ABCG2. ALA is a natural amino acid synthesized in the mitochondria from succinyl-CoA and glycine. Exogenous ALA is imported into the cytoplasm through PEPT-1 and then metabolized to PpIX, which is the final metabolite in the heme biosynthesis pathway.[15] Accumulation of PpIX in the mitochondria would be accelerated by endogenous ALA production, exogenous ALA absorption through PEPT-1, ALA metabolism by heme biosynthesis enzymes and import of ALA metabolite from cytosol into mitochondria through ABCB6, whereas it would be suppressed by metabolism of PpIX to heme by FECH and PpIX elimination through ABCG2. Previous investigations have revealed that PPOX was highly expressed in the ALA-reactive gastric cancer, reflecting the accelerated metabolism of exogenous ALA to PpIX,[16] and that altered expression of PEPT-1 and ABCG2 in gastric cancer cells affected intracellular photosensitizing PpIX levels.[17, 18] In addition, PEPT-1 is reported to be expressed in pancreatic cancer cell lines,[19, 20] and ALA uptake is possibly associated with the efficacy of PDD.[21] However, despite various heme enzymes and membrane transporters affect the PpIX accumulation within the mitochondria, the detailed mechanism of accumulation of this metabolite in pancreatic cancer cells remains unclear. Therefore, we aimed to investigate the molecular mechanisms that influence the fluorescence in ALA-PDD, in particular, the enzymes and membrane transporters involved in the heme biosynthesis pathway in human pancreatic cancer cells.

MATERIALS AND METHODS

Cell lines and cell culture

Immortalized human pancreatic duct epithelial cells (hPDECs) (Applied Biological Materials Inc., Richmond, Canada) and the human pancreatic cancer cell lines MIA PaCa-2, AsPC-1, BxPC-3, SUIT-2, KP-4, KP-3L, TYPK-1 (The Japanese Collection of Research Bioresources, Tokyo, Japan), Capan-1 (Cell Lines Service GmbH, Eppelheim, Germany), and PANC-1 (The European Collection of Cell Cultures, Salisbury, UK) were used in this study. hPDECs were maintained in Prigrow I medium supplemented with 20% fetal bovine serum (FBS). AsPC-1, BxPC-3, KP-3L, and Capan-1 cells were maintained in RPMI 1640 medium supplemented with 10% FBS. MIA PaCa-2 cells were maintained in RPMI 1640 medium supplemented with 10% FBS and non-essential amino acids. SUIT-2 cells were maintained in Eagle's minimal essential medium supplemented with 10% FBS. KP-4 cells were maintained in Iscove's Modified Dulbecco's Medium supplemented with 20% FBS. PANC-1 cells were

Table 1. Primer sequences for quantitative reverse transcription-PCR

Symbol	Forward primer	Reverse primer
PEPT-1	5'- TCACCTGTGGCGAAGTGGTC -3'	5'- GCCACGATGAGCACAATGATG -3'
ABCB6	5'- TTCACTGTGATGCCTGGACAGA -3'	5'- GGATGCAGCCAGAGCTGATG -3'
ABCG2	5'- GCAACCATCAATTCAGGTCAAGA -3'	5'- GAAACACAACACTTGGCTGTAGCA -3'
PBGS	5'-AACCAGCATAAATACTGCCTGAGGA -3'	5'- TGGCACCTCTAGCAGTCAGGAA -3'
PBGD	5'-AACAGCCCAAAGATGAGAGTGATTC -3'	5'- AATGTTGCCACCACACTGTCC -3'
UROS	5'- CCTGAACAGCTACTATTCCGAGCA -3'	5'- CTTGAGACTGTATGTGAGGCCAGAG -3'
UROD	5'- CCCTGTGCCTTGTATGCATCTG -3'	5'- TGTAGCGATGTGGTCCAAAGTCA -3'
CPOX	5'- CACTCCAGGATCCAGAATTGAAAG -3'	5'- TGCATCAACGCACCCAGTC -3'
PPOX	5'- GCCCTTGAAACCCACCTGACTA -3'	5'- ACTAATAACGTGGTCAGCCTCCAGA -3'
FECH	5'- AGGCCATTAAGATGGATGTTGGAA -3'	5'- CTGTCAGAGTGAAGGCTCACAAGAA -3'
β-actin	5'- GCATCCTCACCCTGAAGTA -3'	5'- TGTGGTGCCAGATTTTCTCC -3'

ABC, the ATP-binding cassette; CPOX, coproporphyrinogen oxidase; FECH, ferrochelatase; PBGD, porphobilinogen deaminase; PBGS, porphobilinogen synthase; PEPT-1, oligopeptide transporter-1; PPOX, protoporphyrinogen IX oxidase; UROD, uroporphyrinogen III decarboxylase; UROS, uroporphyrinogen III synthase.

maintained in Dulbecco's modified Eagle's medium (DMEM) supplemented with 10% FBS. TYPK-1 cells were maintained in F12/DMEM supplemented with 5% FBS. All media contained 1% L-glutamine. Cells were cultured in tissue culture dishes at 37°C in a humidified atmosphere of 95% air and 5% carbon dioxide.

Gene expression analysis

Total RNA was extracted from the cells using the miRNeasy Mini Kit (QIAGEN Co., Ltd., Tokyo, Japan) following the manufacturer's instructions. The concentrations of all RNA samples were quantified using the NanoDrop 1000 spectrophotometer (Thermo Fisher Scientific Inc., Tokyo, Japan). Extracted RNA samples were stored at –80°C until further use. The cDNA was prepared from total RNA using the High Capacity cDNA Reverse Transcription Kit (Thermo Fisher Scientific Inc., Tokyo, Japan). The reverse transcription (RT) reactions were performed in aliquots containing 3000 ng of total RNA, 1× RT buffer, 6 mM dNTP mix, 1× RT random primer, 75 units of MultiScribe Reverse Transcriptase, 30 units of RNase inhibitor, and nuclease-free water in a volume of 30 μL at 25°C for 10 min, followed by an incubation at 37°C for 120 min and 85°C for 5 min. A quantitative PCR reaction was performed in 20-μL aliquots containing 1 μL of RT products with 4 μL of LightCycler® FastStart DNA MasterPLUS SYBR Green I (Roche Diagnostics Co., Ltd., Tokyo, Japan), 0.5 μM of each primer, and 14.6 μL of nuclease-free water in the Real-time PCR LightCycler 1.5 Complete System (Roche Diagnostics Co., Ltd., Tokyo, Japan). mRNA levels of PBGS, PBGD, UROS, UROD, CPOX, PPOX, FECH, PEPT-1, ABCB6, and ABCG2 were measured by performing quantitative RT-PCR. Thermal cycling was initiated with a first denaturation step at 95°C for 10 min, followed by 45 cycles of 95°C for 10 s, 60°C for 10 s, and 72°C for 10 s. The cycle passing threshold (Ct) was recorded for mRNA by the LightCycler Software version 3.5.28 (Roche Diagnostics Co., Ltd., Tokyo, Japan), and β-actin was used as the endogenous control for data normalization. Relative expression was calculated using the formula $2^{-\Delta\Delta Ct} = 2 - (\Delta Ct, \text{reagent treatment} - \Delta Ct, \text{control})$.[22] The forward and reverse primer sequences used in this study are summarized in Table 1.

Western blot analysis

The rabbit polyclonal anti-PEPT-1 antibody (Abcam PLC., Tokyo, Japan), rabbit monoclonal anti-β-actin (D6A8) antibody (CST Japan Co., Ltd, Tokyo, Japan), and horseradish peroxidase (HRP)-conjugated goat anti-rabbit IgG H&L (Abcam PLC., Tokyo, Japan) were used. Cultured cells were directly lysed for 15 min on ice using the RIPA Lysis and Extraction Buffer (Thermo Fisher Scientific Inc., Tokyo, Japan) containing cOmplete™ ULTRA Tablets, Mini, EASYpack Protease Inhibitor Cocktail and PhoSTOP (Roche Diagnostics Co., Ltd., Tokyo, Japan). After centrifugation at 21,500 × g for 15 min, protein concentrations were measured using the Pierce 660 nm Protein Assay Reagent (Thermo Fisher Scientific Inc., Tokyo, Japan), and the protein was denatured by boiling for 5 min. The extracted proteins were loaded onto sodium dodecyl sulfate-polyacrylamide gels for electrophoresis and then transferred onto nitrocellulose membranes. After

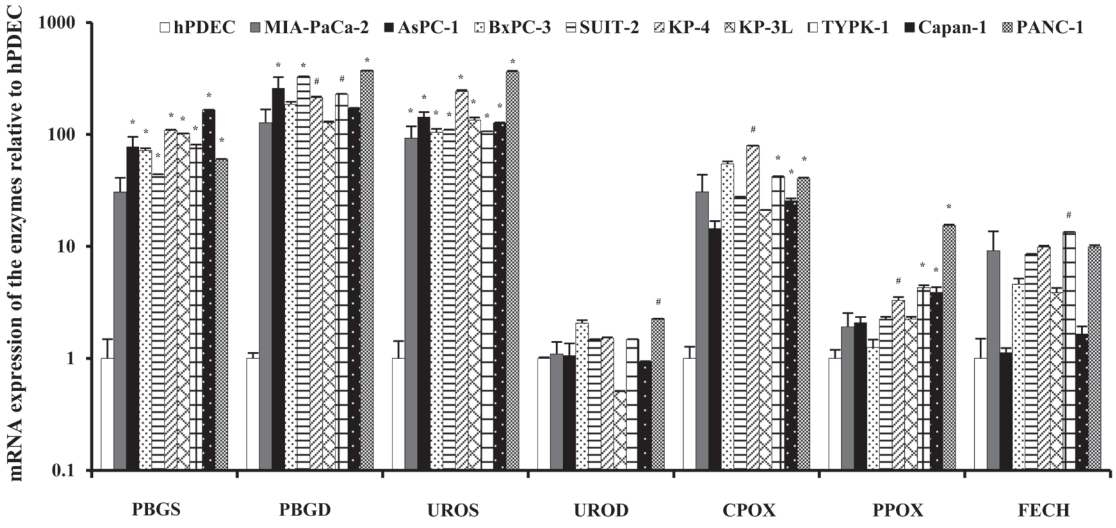

Fig. 2. mRNA expression of heme biosynthesis enzymes in hPDECs and pancreatic cancer cells. The relative mRNA expression levels of the enzymes including PBGS, PBGD, UROS, UROD, CPOX, PPOX, and FECH were assessed using quantitative reverse transcription-polymerase chain reaction in hPDECs and pancreatic cancer cells. The relative levels of enzymes compared to those of hPDECs are shown with a logarithmic scale. Bars indicate average ± SEM. # $P < 0.05$, *$P < 0.01$ compared to the expression levels in hPDECs analyzed by one-way ANOVA followed by post hoc Dunnet test. CPOX, coproporphyrinogen oxidase; FECH, ferrochelatase; hPDEC, human pancreatic duct epithelial cell; PBGD, porphobilinogen deaminase; PBGS, porphobilinogen synthase; PPOX, protoporphyrinogen IX oxidase; UROD, uroporphyrinogen III decarboxylase; UROS, uroporphyrinogen III synthase.

blocking with 5% milk in TBST (150 mmol/L NaCl and 50 mmol/L Tris-HCl containing 0.05% Tween-20), the membranes were incubated with anti-PEPT-1 (1:500 dilution) or anti-β-actin (1:1000 dilution) antibodies at 4°C overnight. After washing with TBST 3 times (5 min each), the membranes were incubated with their corresponding HRP-conjugated secondary antibodies (for PEPT-1, 1:5000 dilution; for β-actin, 1:20,000 dilution) at room temperature for 1 h. After washing with TBST 3 times (5 min each), the bound antibodies were visualized using the Clarity Western ECL Substrate (Bio-Rad Laboratories, Inc., Tokyo, Japan) and an image analyzer (LAS-3000 mini, Fujifilm Co. Ltd., Tokyo, Japan). The band intensities were quantified using the Multi Gauge Ver. 3.1 (Fujifilm Co. Ltd., Tokyo, Japan).

Incubation of cells with ALA

ALA hydrochloride (Cosmo Bio Co., Ltd., Tokyo, Japan) was added to the culture medium and the cells were incubated in the dark. The cells were then harvested for RNA quantification or examined for fluorescence analyses. Fluorescence was examined using a BZ-X710 microscope (Keyence, Osaka, Japan) with an excitation wavelength of 405 nm, and fluorescence detection at 630 nm, with a 40× objective. Fluorescence intensity after ALA administration was quantified as previously described.[23] In brief, all detectable cells were outlined, and the intensity of each cell was analyzed using ImageJ software (U. S. National Institutes of Health, Bethesda, MD). Fluorescence intensity as reported was an average of the intensities of all analyzed cells. For the transporter inhibition experiment, P-(aminomethyl) benzoic acid (AMBA; FUJIFILM Wako Pure Chemical Co., Ltd., Osaka, Japan), a PEPT-1 inhibitor, was added to the culture medium to a final concentration of 30 mM.

Statistical analysis

The expression levels of mRNA for enzymes and transporters were analyzed by one-way analysis of variance (ANOVA) with post hoc Dunnett test. The unpaired t test was performed to assess the differences in mRNA expressions after ALA administration. The differences in signal intensities in western blot analysis and fluorescent intensities between each group were analyzed by one-way ANOVA with post hoc Tukey test. P values less than 0.05 were considered as significant. StatFlex (Windows ver. 6.0; Arthech, Osaka, Japan) was used for the statistical analysis. All values are expressed as the mean ± SEM.

RESULTS

mRNA expression of heme biosynthesis enzymes and membrane transporters

Most of the mRNA expression levels of the heme biosynthesis enzymes were higher in pancreatic cancer cells than in hPDEC cells; however, variations in the

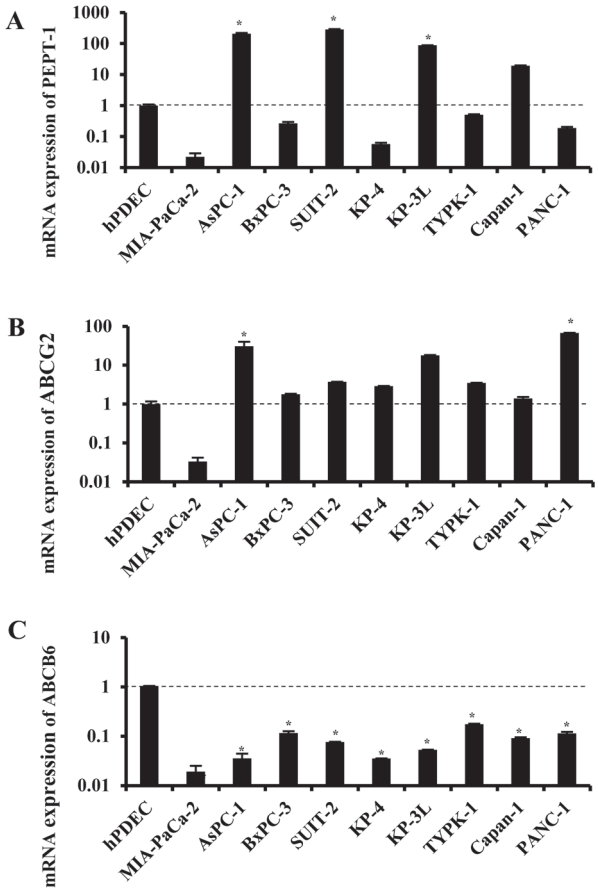

Fig. 3. mRNA expression levels of membrane transporters. The relative mRNA expression levels of (**A**) PEPT-1, (**B**) ABCG2, and (**C**) ABCB6 assessed using quantitative reverse transcription-polymerase chain reaction in hPDECs and pancreatic cancer cells. The relative levels compared to hPDECs are shown with a logarithmic scale. Bars indicate average ± SEM. **P* < 0.01 compared to the expression levels in hPDECs analyzed by one-way ANOVA followed by post hoc Dunnet test. ABC, the ATP-binding cassette; hPDEC, human pancreatic duct epithelial cell; PEPT-1, oligopeptide transporter-1.

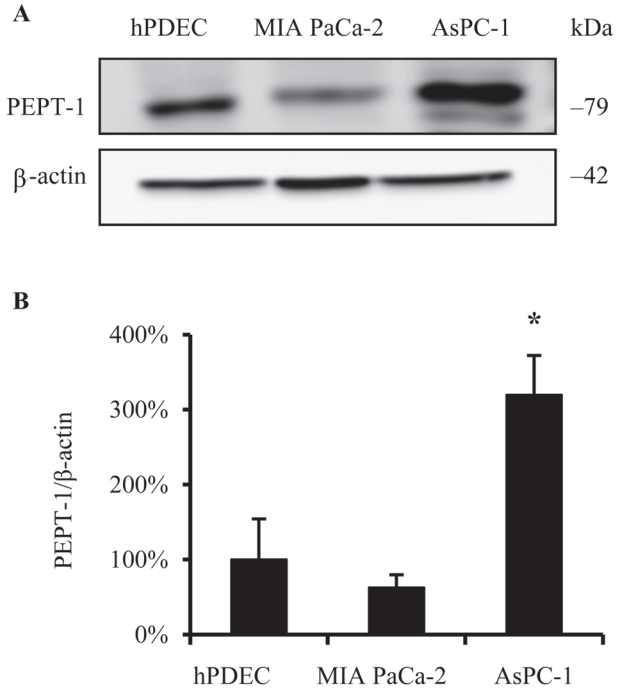

Fig. 4. Protein expression levels of PEPT-1 in hPDECs, MIA PaCa-2, and AsPC-1 cells. (**A**) Representative image of western blot for PEPT-1 and β-actin in hPDECs, MIA PaCa-2, and AsPC-1 cells. (**B**) Quantitative analyses of the western blots for PEPT-1 protein from 3 repetitive experiments. The signal intensity was normalized to the β-actin protein level and expressed as relative expression levels in hPDECs. Bars indicate average ± SEM. **P* < 0.05 compared to hPDECs. One-way ANOVA followed by post hoc Tukey test. hPDEC, human pancreatic duct epithelial cell; PEPT-1, oligopeptide transporter-1.

mRNA levels among cancer cells were relatively small (Fig. 2). mRNA expression of membrane transporters, in particular for PEPT-1, in pancreatic cancer cells showed remarkable differences; PEPT-1 levels were significantly higher in AsPC-1, SUIT-2 and KP-3L than in hPDECs and showed lower trend in MIA PaCa-2, BxPC-3, KP-4, TYPK-1 and PANC-1 than in hPDECs (Fig. 3A). Most of the cancer cells, except for MIA PaCa-2, showed higher levels of ABCG2 (Fig. 3B). The expressions of ABCB6 were low in all the pancreatic cancer cells compared to hPDECs (Fig. 3C).

Protein expression of PEPT-1

As PEPT-1 could be involved in PpIX overexpression,[14] we further investigated the protein levels of PEPT-1 in the hPDECs, MIA PaCa-2, and AsPC-1 cells, which showed remarkable differences in the quantitative RT-PCR analyses. PEPT-1 was abundantly expressed in AsPC-1 cells compared to the expression in hPDECs, in contrast to the weak expression in MIA PaCa-2 cells (Fig. 4A). Quantitative analysis of the western blot revealed that the difference between hPDECs and AsPC-1 cells was significant (Fig. 4B).

Fluorescence after incubation with ALA

The results from quantitative RT-PCR and western blot suggested that the increased expression of PEPT-1 could reveal key mechanisms in ALA-PDD. Therefore, we investigated the fluorescence in hPDECs, MIA PaCa-2 and AsPC-1 cells after ALA administration. The fluorescence was analyzed in the time course at 1, 2, and 4 h after ALA administration (Fig. 5). AsPC-1 cells, which highly expressed PEPT-1, showed a stronger and rapid induction of fluorescence than hPDECs or MIA PaCa-2 cells. This result suggests that the ability to distinguish cancer cells and hPDECs was stronger at an earlier

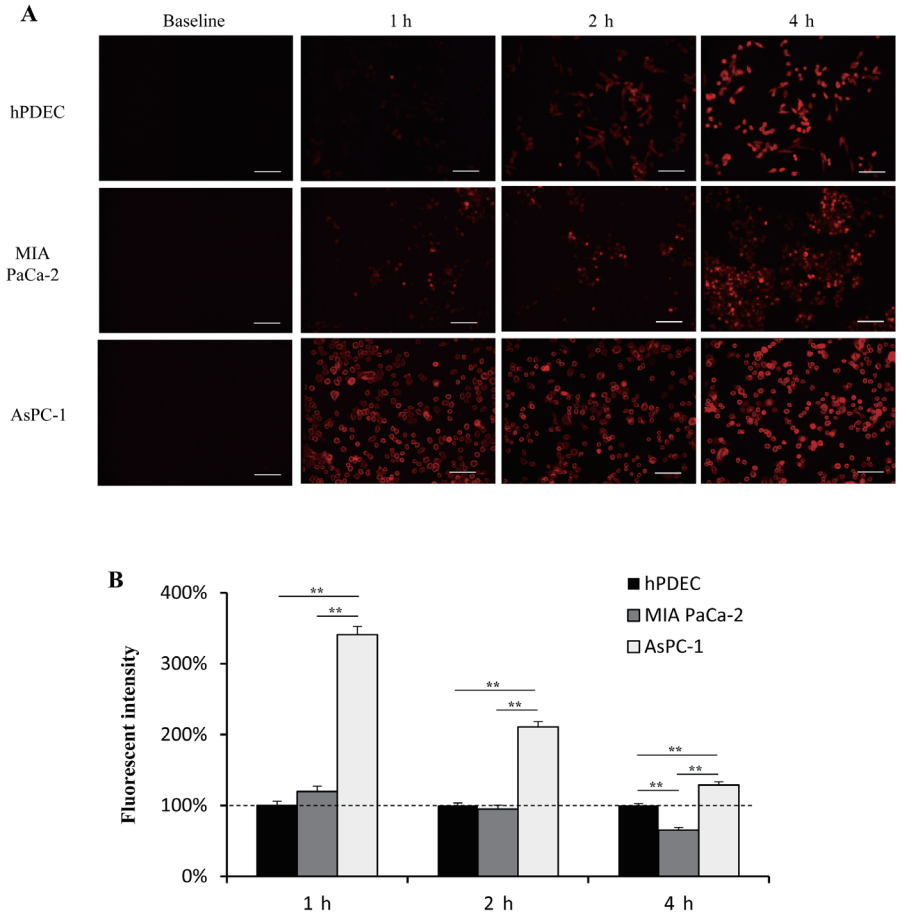

Fig. 5. Fluorescence in hPDECs, MIA PaCa-2, and AsPC-1 cells after incubation with ALA. (**A**) Representative images of fluorescence in hPDECs, MIA PaCa-2, and AsPC-1 cells at baseline, 1, 2, and 4 h after ALA administration. ALA was administered at final concentrations of 0.25 mM. Bar = 100 μm. (**B**) Fluorescence intensities were quantified and represented as the relative intensity to hPDECs. Bars indicate average ± SEM. $^{**}P < 0.01$ (one-way ANOVA with post hoc Bonferroni test). ALA, 5-aminolevulinic acid; hPDEC, human pancreatic duct epithelial cell.

time-point. Inhibition of PEPT-1 by AMBA attenuated PpIX accumulation in all the cells, especially in AsPC-1 cells (Fig. 6). Since several cell lines other than AsPC-1 showed high mRNA expression of PEPT-1 as well, we further investigated the PpIX accumulation in the other cell lines. The cell lines with relatively high expression of PEPT-1 such as SUIT-2, KP-3L, and Capan-1 showed intense fluorescent compared to the other cell lines with relatively low expression of PEPT-1 such as BxPC-3, KP-4, TYPI-1, and PANC-1 (Fig. 7).

DISCUSSION

In this study, we demonstrate that PEPT-1, which regulates the cellular intake of ALA, was highly expressed in AsPC-1 cells compared to the expression in hPDECs or the pancreatic cancer cell lines MIA PaCa-2. AsPC-1 cells showed intense fluorescence after ALA administration, which was attenuated by the PEPT-1 inhibitor. Pancreatic cancer cells expressing high level of PEPT-1 showed strong fluorescent by the administration of ALA. These data suggest that PEPT-1 was associated with the intensity of ALA-induced fluorescence in pancreatic cancer cells.

ALA-PDD is a promising diagnostic modality for diagnosing cancers. This technique was applied in the diagnosis of bladder, brain, and gastric tumors,[11, 13, 16] and is expected to contribute to the early diagnosis of pancreatic cancer. Harada et al. reported that ALA-PDD was useful for detecting peritoneal metastasis during staging laparoscopy in patients with pancreatic cancer.[24] The diagnosis of pancreatic cancer at an early stage is still challenging, and the development of a new modality for a more accurate diagnosis is needed. Cytodiagnosis or histological diagnosis using endoscopic ultrasound-guided fine needle aspiration (EUS-FNA) is one of the modalities that can be utilized for the early and accurate diagnosis of pancreatic cancer. EUS-FNA usually requires an on-site review by a cytopathologist

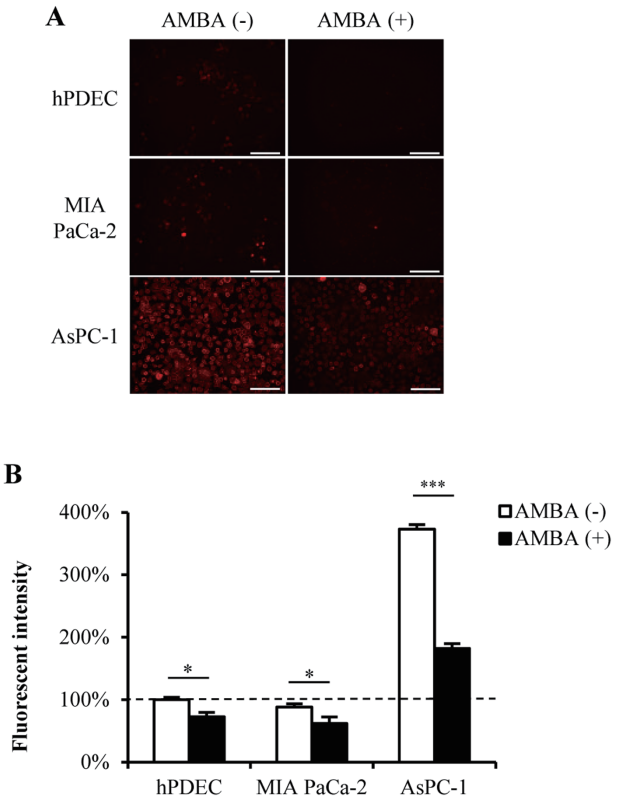

Fig. 6. PpIX accumulation in hPDECs, MIA PaCa-2, and AsPC-1 cells incubated with ALA and the PEPT-1 inhibitor P-(aminomethyl) benzoic acid. (**A**) Representative images of fluorescence in hPDECs, MIA PaCa-2, and AsPC-1 cells after ALA administration with or without AMBA at a final concentration of 30 mM. Bar = 200 μm. (**B**) Quantitative analyses for fluorescence intensities in hPDECs, MIA PaCa-2, and AsPC-1 cells, expresses as the relative intensity to hPDECs without AMBA. Bars in dicate average ± SEM. $*P < 0.05$, $***P < 0.001$ (Mann-Whitney *U* test in each cell line). ALA, 5-aminolevulinic acid; hPDEC, human pancreatic duct epithelial cell.

or cytotechnician. Although the diagnostic accuracy relies on the adequacy of the samples, a cytopathologist or cytotechnician cannot always stay on-site during the procedure to review the samples. EUS-FNA using ALA-PDD may allow for diagnosing pancreatic cancer more easily. The underlying mechanism for the tumor-specific fluorescence has not been fully understood. Therefore, it will contribute to the accurate diagnosis or detection of pancreatic cancer to elucidate the mechanism of ALA-PDD in pancreatic cancer cells.

In the present study, we investigated the association of heme metabolism enzymes and transporters to ALA-PDD in pancreatic cancer cells. In contrast to the small variations in expression level of heme enzymes, membrane transporters such as PEPT-1 and ABCG2 showed significant differences among the cancer cell lines. Both of these two transporters were highly expressed in AsPC-1 cells, and weakly expressed in MIA PaCa-2 cells compared to the normal cells. Therefore, we hypothesized that a comparison of PpIX accumulation in these cell lines would reveal the relevant transporters mediating PpIX accumulation; PEPT-1 would be dominant if PpIX accumulation was high in AsPC-1 cells, and ABCG2 would be dominant if PpIX accumulation was low in AsPC-1 cells. Upon ALA administration, AsPC-1 cells showed rapid induction and intense fluorescence, indicating a considerable role of PEPT-1 in ALA-mediated PpIX accumulation. The influence of endogenous ALA production on ALA-PDD could be ignored, because the fluorescence was almost undetectable in the absence of ALA administration. We have also investigated the PpIX accumulation in all the pancreatic cancer cell lines. The cell lines with relatively high expression of PEPT-1 showed intense fluorescent after ALA administration, suggesting that PEPT-1 plays an important role in accumulation of PpIX in pancreatic cancer. We further confirmed the relationship of PEPT-1 and ALA-mediated PpIX accumulation using the PEPT-1 inhibitor AMBA, which attenuated PpIX accumulation especially in AsPC-1. In a previous report, FECH has been reported to enhance the fluorescence after the administration of ALA.[25] Since the expression of FECH was higher in MIA PaCa-2 than in AsPC-1 in this study, we could not eliminate the influence of FECH to the difference between AsPC-1 and MIA PaCa-2. However, we revealed that the fluorescence in hPDECs and AsPC-1 remarkably differ despite the nearly similar expression levels of FECH in these two cell lines. Therefore, we consider the influence of FECH to the ALA-induced fluorescence is relatively weak compared to PEPT-1. Previous investigations in gastric cancer showed the relationship between PPOX and ALA-induced fluorescence.[16] The expressions level of PPOX in pancreatic cancer is similar to that in gastric cancer, therefore PPOX might affect the PpIX accumulation in AsPC-1 as well.[26] However, as we have discussed above, exogenously administered ALA and ALA absorption through PEPT-1 play an important role in ALA-induced PDD in pancreatic cancer. Together with the fact that MIA PaCa-2 cells, which expressed relatively low level of PEPT-1, showed weak induction of fluorescence suggests that ALA-PDD depends on the membrane transporters expressed in each cancer. AsPC-1 derives from metastatic pancreatic cancers, while MIA PaCa-2 cells derives from pancreatic tumor tissue. We speculate that the expression levels of PEPT-1 depend on the degree of malignancy. In fact, it has been proved that PEPT-1 promotes the progression or proliferation of pancreatic cancer.[27] Further investigations,

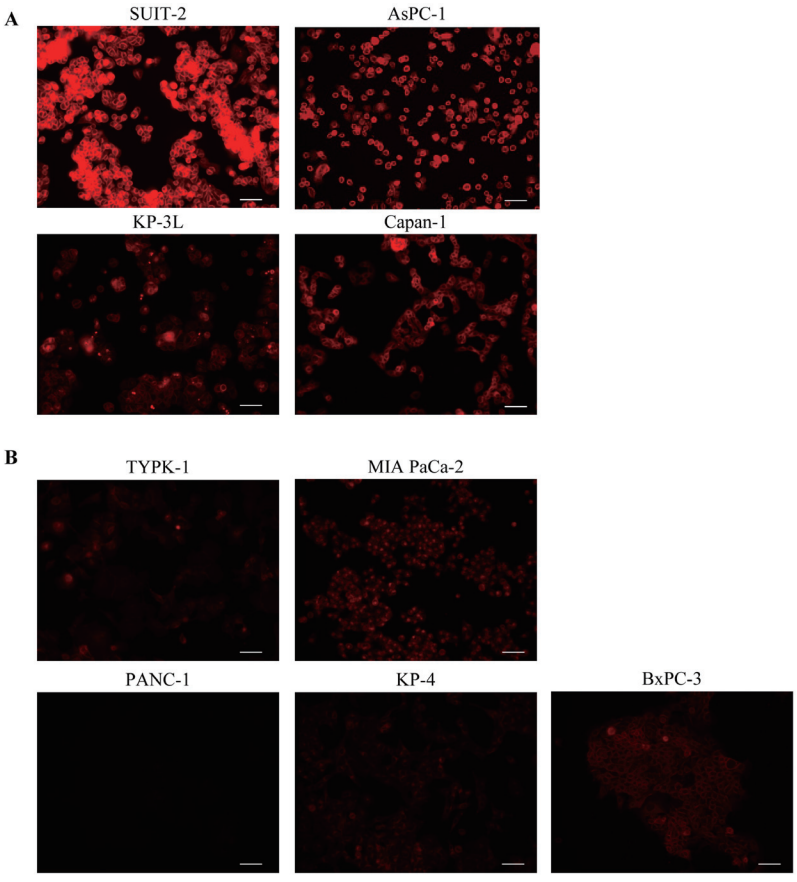

Fig. 7. PpIX accumulation in pancreatic cancer cell lines after administration of ALA. (**A**) Representative images of fluorescence in pancreatic cancer cell lines with relatively high expression of PEPT-1. Images were captured 1 h after the administration of ALA in SUIT-2, AsPC-1, KP-3L, and Capan-1 cells. (**B**) Representative images of fluorescence in cell lines with relatively low expression of PEPT-1. Images were captured 1 h after the administration of ALA in TYPK-1, MIA PaCa-2, PANC-1, KP-4, and BxPC-3 cells. Bar = 100 μm.

especially with clinical samples, are required to apply this technique to clinical specimens.

There were some limitations in this study. Some porphyrins synthesized in the ALA-to-PpIX pathway might also emit fluorescence, thereby influencing the results. However, the fluorescence spectrum of the porphyrin intermediate metabolite is different from that of PpIX. This discrepancy in the spectrum has been applied in the diagnosis of porphyria.[28] Expression levels of heme enzymes among the cancer cell lines were not downregulated. Therefore, we assumed that the influence of fluorescence from the other porphyrins was negligible. ABCG2, an exporter of PpIX, may be another factor for ALA-induced fluorescence. However, as we have discussed above, the fluorescence was remarkably stronger in AsPC-1 compared to MIA PaCa-2 cells, suggesting that PEPT-1 contributed dominantly to the ALA-induced PpIX accumulation. We did not measure the expression level of ALAS, which mediates endogenous ALA production. However, endogenous ALA production or the expression of ALAS could be ignored because of the faint autofluorescence observed in the absence of ALA.

In conclusion, we report a new finding for the mechanism of ALA-PDD in pancreatic cancer cells. Cells with high expression levels of PEPT-1 could be easily distinguished from normal cells via ALA administration. These findings contribute to the development of a novel diagnostic modality, ALA-PDD, for pancreatic cancer.

The authors declare no conflict of interest.

REFERENCES

1 Gall TMH, Tsakok M, Wasan H, Jiao LR. Pancreatic cancer: current management and treatment strategies. Postgrad Med J. 2015;91:601-7. DOI: 10.1136/postgradmedj-2014-133222, PMID: 26243882

2 Michl P, Pauls S, Gress TM. Evidence-based diagnosis and staging of pancreatic cancer. Best Pract Res Clin Gastroenterol. 2006;20:227-51. DOI: 10.1016/j.bpg.2005.10.005, PMID: 16549326

3 Wolfgang CL, Herman JM, Laheru DA, Klein AP, Erdek MA, Fishman EK, et al. Recent progress in pancreatic cancer. CA Cancer J Clin. 2013;63:318-48. DOI: 10.3322/caac.21190, PMID: 23856911

4 Pietryga JA, Morgan DE. Imaging preoperatively for pancreatic adenocarcinoma. J Gastrointest Oncol. 2015;6:343-57. PMID: 26261722

5 Baekelandt BMG, Hjermstad MJ, Nordby T, Fagerland MW, Kure EH, Heiberg T, et al. Preoperative cognitive function predicts survival in patients with resectable pancreatic ductal adenocarcinoma. HPB (Oxford). 2016;18:247-54. DOI: 10.1016/j.hpb.2015.09.004, PMID: 27017164

6 Gillen S, Schuster T, Meyer zum Büschenfelde C, Friess H, Kleeff J. Preoperative/neoadjuvant therapy in pancreatic cancer: a systematic review and meta-analysis of response and resection percentages. PLoS Med. 2010;7:e1000267. DOI: 10.1371/journal.pmed.1000267, PMID: 20422030

7 Hartwig W, Hackert T, Hinz U, Gluth A, Bergmann F, Strobel O, et al. Pancreatic cancer surgery in the new millennium: better prediction of outcome. Ann Surg. 2011;254:311-9. DOI: 10.1097/SLA.0b013e31821fd334, PMID: 21606835

8 He J, Ahuja N, Makary MA, Cameron JL, Eckhauser FE, Choti MA, et al. 2564 resected periampullary adenocarcinomas at a single institution: trends over three decades. HPB (Oxford). 2014;16:83-90. DOI: 10.1111/hpb.12078, PMID: 23472829

9 Egawa S, Toma H, Ohigashi H, Okusaka T, Nakao A, Hatori T, et al. Japan pancreatic cancer registry; 30th year anniversary: Japan Pancreas Society. Pancreas. 2012;41:985-92. DOI: 10.1097/MPA.0b013e318258055c, PMID: 22750974

10 Inoue Y, Tanaka R, Komeda K, Hirokawa F, Hayashi M, Uchiyama K. Fluorescence detection of malignant liver tumors using 5-aminolevulinic acid-mediated photodynamic diagnosis: principles, technique, and clinical experience. World J Surg. 2014;38:1786-94. DOI: 10.1007/s00268-014-2463-9, PMID: 24493071

11 Ishikawa T, Takahashi K, Ikeda N, Kajimoto Y, Hagiya Y, Ogura S, et al. Transporter-mediated drug interaction strategy for 5-aminolevulinic acid (ALA)-based photodynamic diagnosis of malignant brain tumor: molecular design of ABCG2 inhibitors. Pharmaceutics. 2011;3:615-35. DOI: 10.3390/pharmaceutics3030615

12 Kishi K, Fujiwara Y, Yano M, Inoue M, Miyashiro I, Motoori M, et al. Staging laparoscopy using ALA-mediated photodynamic diagnosis improves the detection of peritoneal metastases in advanced gastric cancer. J Surg Oncol. 2012;106:294-8. DOI: 10.1002/jso.23075, PMID: 22389064

13 Lopez A, Liao JC. Emerging endoscopic imaging technologies for bladder cancer detection. Curr Urol Rep. 2014;15:406. DOI: 10.1007/s11934-014-0406-5, PMID: 24658832

14 Ajioka RS, Phillips JD, Kushner JP. Biosynthesis of heme in mammals. Biochimica et Biophysica Acta (BBA) - Molecular Cell Research. 2006;1763:723-36. DOI: 10.1016/j.bbamcr.2006.05.005, PMID: 16839620

15 Hinnen P, de Rooij FW, Terlouw EM, Edixhoven A, van Dekken H, van Hillegersberg R, et al. Porphyrin biosynthesis in human Barrett's oesophagus and adenocarcinoma after ingestion of 5-aminolaevulinic acid. Br J Cancer. 2000;83:539-43. DOI: 10.1054/bjoc.2000.1300, PMID: 10945504

16 Kurumi H, Kanda T, Kawaguchi K, Yashima K, Koda H, Ogihara K, et al. Protoporphyrinogen oxidase is involved in the fluorescence intensity of 5-aminolevulinic acid-mediated laser-based photodynamic endoscopic diagnosis for early gastric cancer. Photodiagn Photodyn Ther. 2018;22:79-85. DOI: 10.1016/j.pdpdt.2018.02.005, PMID: 29425880

17 Kobuchi H, Moriya K, Ogino T, Fujita H, Inoue K, Shuin T, et al. Mitochondrial localization of ABC transporter ABCG2 and its function in 5-aminolevulinic acid-mediated protoporphyrin IX accumulation. PLoS One. 2012;7:e50082. DOI: 10.1371/journal.pone.0050082, PMID: 23189181

18 Hagiya Y, Endo Y, Yonemura Y, Takahashi K, Ishizuka M, Abe F, et al. Pivotal roles of peptide transporter PEPT1 and ATP-binding cassette (ABC) transporter ABCG2 in 5-aminolevulinic acid (ALA)-based photocytotoxicity of gastric cancer cells in vitro. Photodiagn Photodyn Ther. 2012;9:204-14. DOI: 10.1016/j.pdpdt.2011.12.004, PMID: 22959800

19 Gonzalez DE, Covitz KM, Sadée W, Mrsny RJ. An oligopeptide transporter is expressed at high levels in the pancreatic carcinoma cell lines AsPc-1 and Capan-2. Cancer Res. 1998;58:519-25. PMID: 9458100

20 Mitsuoka K, Miyoshi S, Kato Y, Murakami Y, Utsumi R, Kubo Y, et al. Cancer detection using a PET tracer, 11C-glycylsarcosine, targeted to H+/peptide transporter. J Nucl Med. 2008;49:615-22. DOI: 10.2967/jnumed.107.048231, PMID: 18344442

21 Zimmermann M, Kappert K, Stan AC. U373-MG cells express PepT2 and accumulate the fluorescently tagged dipeptide-derivative β-Ala-Lys-Nε-AMCA. Neurosci Lett. 2010;486:174-8. DOI: 10.1016/j.neulet.2010.09.046, PMID: 20868728

22 Livak KJ, Schmittgen TD. Analysis of relative gene expression data using real-time quantitative PCR and the 2(-Δ Δ C(T)) Method. Methods. 2001;25:402-8. DOI: 10.1006/meth.2001.1262, PMID: 11846609

23 Tokonami N, Takata T, Beyeler J, Ehrbar I, Yoshifuji A, Christensen EI, et al. Uromodulin is expressed in the distal convoluted tubule, where it is critical for regulation of the sodium chloride cotransporter NCC. Kidney Int. 2018;94:701-15. DOI: 10.1016/j.kint.2018.04.021, PMID: 30007527

24 Harada K, Murayama Y, Kubo H, Matsuo H, Morimura R, Ikoma H, et al. Photodynamic diagnosis of peritoneal metastasis in human pancreatic cancer using 5-aminolevulinic acid during staging laparoscopy. Oncol Lett. 2018;16:821-8. DOI: 10.3892/ol.2018.8732, PMID: 29963150

25 Fukuhara H, Inoue K, Kurabayashi A, Furihata M, Fujita H, Utsumi K, et al. The inhibition of ferrochelatase enhances 5-aminolevulinic acid-based photodynamic action for prostate cancer. Photodiagn Photodyn Ther. 2013;10:399-409. DOI: 10.1016/j.pdpdt.2013.03.003, PMID: 24284092

26 UniProt Consortium. UniProt: a worldwide hub of protein knowledge. Nucleic Acids Res. 2019;47:D506-15. DOI: 10.1093/nar/gky1049, PMID: 30395287

27 Schniers B, Bhutia Y. PEPT1 as a tumor promoter and novel drug target to treat pancreatic cancer [abstract]. In; Proceedings of the American Association for Cancer Research Annual Meeting 2019; 2019 March 29–April 3; Atlanta, GA. Philadelphia (PA): AACR; Cancer Res 2019;79 Suppl 13.

28 Deacon AC, Elder GH. ACP Best Practice No 165: front line tests for the investigation of suspected porphyria. J Clin Pathol. 2001;54:500-7. DOI: 10.1136/jcp.54.7.500, PMID: 11429419